Microscopic pore structures and controlling factors of the Micro- and Nano- Scale tight sandstone reservoirs in the Western Sichuan Depression, China

Qiaochu Wang*, Dongxia Chen, Bixuan Zhang, Longlong Li
State Key Laboratory for Oil and Gas Resource and Prospecting, Changping Fuxue Road 18, 102249 Beijing, China
* Corresponding author. E-mail address: currywang2@163.com

ABSTRACT

Western Sichuan Depression (abbreviated WSD) has a natural gas resource of about $31646.98\times10^8m^3$, indicating huge exploration potential. However, large amounts of micro- and nano-scale reservoir and the lack of study in microcosmic field restrict the exploration and development of tight sandstone gas. In this study, we choose the samples from the Upper Triassic to Jurassic to analyze their microscopic pore structures with the use of several experiments in quality and quantity.

The result shows reservoirs in WSD have low porosity and permeability. Intergranular pores and intragranular pores are the main pore types in our samples. The main pore radius is from 100 to 150 μm which is much lower than that in conventional reservoirs. The throat type is dominated by reduced-neck throat and sheet-like throat with an average radius of 997.3 nm, throats with radius larger than 1μm are rare. The pore throat relationship is complex for the difference in ratio of pore-throat radius. Diagenesis including compaction, cementation and dissolution are controlling factors of the microscopic structures.

Keywords: tight sandstone gas, microscopic pore structures, micro- and nano- scale reservoirs

1 INTRODUCTION

Tight sandstone has very low porosity and permeability as its basic characteristics because of its geological histories [1]. As a type of hydrocarbon reservoir, multi-stage diagenesis and strong reform lead to complex pore structure then determine their capacity to flow and reserve oil and gas.

To analyze microscopic pore structures, several laboratory techniques can be applied. Cast thin section is the most regular method to observe pore shapes and types in millimeter scale [2].

Scanning electron microscopy (SEM) enabled imaging of micro- and nano- scale pore bodies and throats [3]. Micro- CT scan can be used to observe shape of throats in reservoirs [4]. Constant-rate mercury injection techniques can quantify the pore and throat distribution respectively [5].

Tight sandstone gas exploration and development is becoming more and more important in China because of its giant resource potential. Western Sichuan Depression has a natural gas resource of about $31646.98\times10^8m^3$. Tight sandstone gas resource is abundant in this area. In this study, we choose the samples from the Upper Triassic to Jurassic to analyze their microscopic pore characteristics with the use of cast thin section, scanning electron microscopy, micro- CT scan, and constant-rate mercury injection in quality and quantity.

2 METHODOLOGY

2.1 Sample Collection

During late Triassic to Jurassic WSD was mainly in delta sedimentary environment but there are obvious difference of lithologies in different formations [6]. So we choose samples from different formation (Table 1). Among them, 2 samples are from middle-shallow layer of Shaximiao Formation of Jurassic (about 2000 m) and other 7 are from deep layer of the fourth member of Xujiahe Formation (3700~3800 m) and the second member of Xujiahe Formation (about 5000 m).

Well	Num	For	D (m)	Φ(%)	P ($\times10^{-3}\mu m^2$)
CF125	6	T_3x^4	3841.9	7.07	0.933
CF125	7	T_3x^4	3841.9	6.48	0.424
CF125	10	T_3x^4	3886.2	6.1	0.751
CX135	15	J_2x	2407.8	8.35	0.236
CH100	35	T_3x^2	5059.6	5.16	0.349
CX455	39	J2x	2293.7	16.75	87.426
CG561	59	T_3x^4	3631.4	5.91	1.049
CG561	60	T_3x^2	4940.2	5.52	0.559
FG21	65	T_3x^4	3774.9	11.81	144.257

Num is sample number, For is formation, D is depth, Φ is porosity of sample, P is permeability of sample.

Table 1: Basic sample materials

2.2 Methodology

2.2.1 Cast Thin Section and Image Analysis

Pores in millimeter scale can be observed by use of cast thin section. Compare to regular thin sections, colored epoxy resin was used to fill the pore bodies so that they will be easily observed and count. Combined with micro image

analysis technology which can seek and edit pixel groups we will get the feature of millimeter scale pore bodies.

2.2.2 Scanning Electron Microscopy

Micro- and nano- scale pore bodies and throats were observed by scanning electron microscopy (SEM) for their shapes and types. In this study we used Quanta-200F SEM which has a resolution of 1.2 nm. Samples were polished to make pore bodies and throats more clear.

2.2.3 Micro-CT Scan

X-ray was used to do large scale scan of rock, then the scan message was dealt with by software to give pore and throat images of the rock sample. Samples were made into cylinders having a diameter of about 1mm and a height of about 2.5 mm.

2.2.4 Constant-Rate Mercury Injection

Constant-rate mercury injection was used to distinguish throat from pore bodies. We can compare the different characteristics of pore bodies and throats and then their relationships by this method.

3 RESULTS

3.1 Pore Body Structure

3.1.1 Pore Types

Pore types were observed by cast thin section with blue epoxy resin. According to the micrograph (Figure 1), the main pore types in our samples are intergranular pore (Figure 1-a,b) and intragranular pore which conclude feldspar intragranular pore (Figure 1-c) and cutting intragranular pore (Figure 1-d).

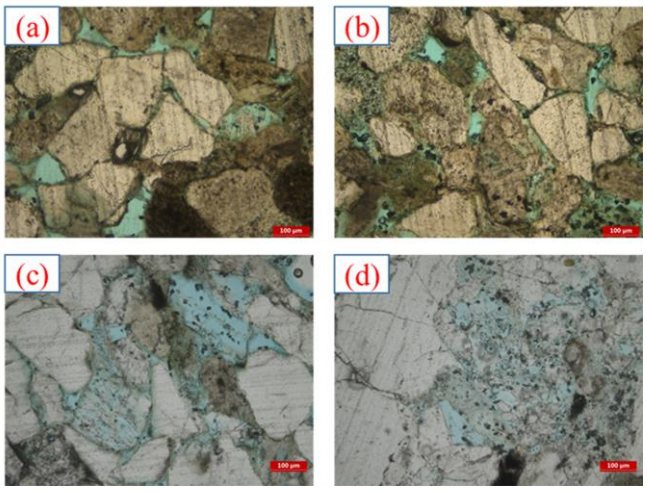

Figure 1: Cast thin section micrographs of samples. (a) Intergranular pores, sample 39. (b) Intergranular pores, sample 65 (c) Feldspar intragranular pore, sample 65. (d) Cutting intragranular pore, sample 65.

3.1.2 Pore Size Distribution

Constant-rate mercury injection can be used to quantify pore size and its distribution in each sample. We can conclude that even though the porosity and permeability are different in samples, their pore sizes are similar. The pore radius average is from 128.51 μm to 165.43 μm with an average of 149.74 μm among all samples (Table 2). As for distribution, the main pore radius distribute from 100 to 150 μm with an average of 58.73%. Few samples have pore radius larger than 250 μm (Figure 2).

Num	For	pore size distributions(%)				Average (μm)
		I	II	III	IV	
6	T_3x^4	2.2	59.0	33.2	5.6	149.3
7	T_3x^4	1.5	52.5	36.2	9.8	157.1
10	T_3x^4	21.2	57.6	15.5	5.7	130.9
15	J_2x	2.8	43.0	33.5	20.7	165.4
35	T_3x^2	2.6	52.1	33.4	11.9	157.5
39	J_2x	2.2	60.6	27.8	9.4	153.9
59	T_3x^4	5.5	87.5	7.0	0.0	128.5
60	T_3x^2	3.4	54.6	33.8	8.2	153.3
65	T_3x^4	1.6	61.7	28.3	8.4	151.9

I: pore radius <100 μm; II: pore radius 100~150 μm; III: pore radius 150~200 μm; IV: pore radius >200 μm

Table 2: Pore size and distributions from constant-rate mercury injection

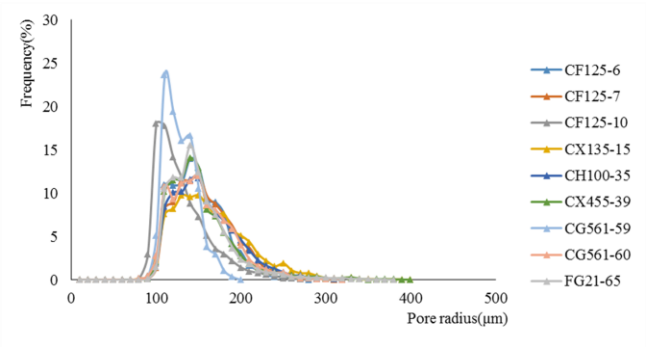

Figure 2: Pore size distributions of 8 samples

3.2 Throat Structures

3.2.1 Throat Types

Previous study shows that throats in reservoirs can be divided into several types based on their shapes [7]. In tight gas reservoirs, throats are much narrower than pores. In our samples, reduced-neck throat and sheet-like throat are dominant throat types while sheet-like throat can be divide into two types according to their bending degree. The shape of throats were observed by SEM and Micro-CT scan (Figure 3).

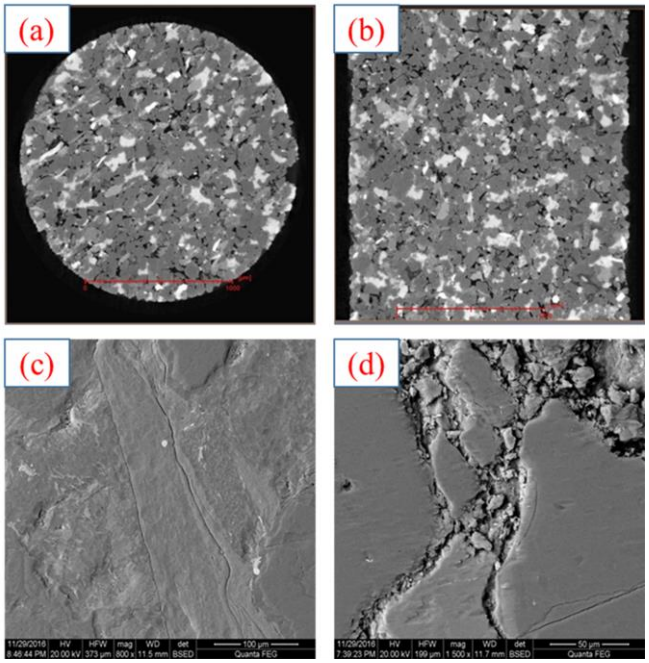

Figure 3: Throat types from SEM and Micro-CT scan. (a) Reduced-neck throat by Micro-CT scan image in XY visual angle, sample 65; (b) Reduced-neck throat by Micro-CT scan image in XZ visual angle, sample 65; (c) Sheet-like throat (straight) by SEM image, sample 65; (d) Sheet-like throat (curved) by SEM, sample 15.

3.2.2 Throat Size Distribution

Throat sizes and their distribution can also be measured by constant-rate mercury injection. From the results, radius of most samples are less than 700 nm (Table 3). Distributions among these samples are quite different, some sample have wide range of throat radius while some samples have concentrated distribution with different peaks (Figure 4).

Num	For	Average (μm)	Main throat radius(μm)	Min (μm)	Max (μm)
6	T_3x^4	0.53	0.47	0.39	0.69
7	T_3x^4	0.52	0.53	0.42	0.74
10	T_3x^4	0.72	0.80	0.62	1.09
15	J_2x	0.58	0.55	0.44	0.92
35	T_3x^2	0.56	0.51	0.44	0.83
39	J_2x	2.34	3.22	2.63	4.17
59	T_3x^4	0.61	0.43	0.34	0.71
60	T_3x^2	0.58	0.63	0.52	1.07
65	T_3x^4	2.45	3.68	3.36	5.44

Table 3: Throat radius data from constant-rate mercury injection

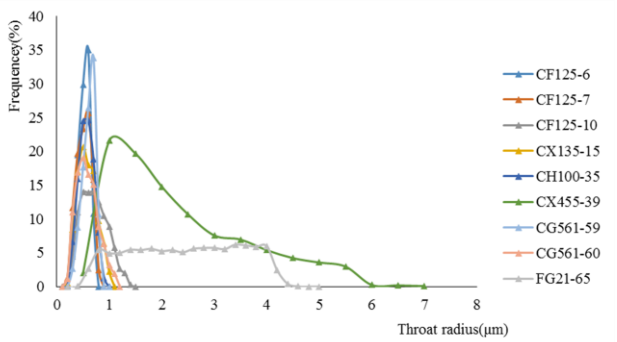

Figure 4: Throat size distributions of 8 samples

3.3 Pore Throat Relationship

Ratio of pore-throat radius (RPTR) is a dominant parameter which mainly reflects the pore throat relationship. In our study, we used constant-rate mercury injection to get the data of RPTR. The result shows that this relationship is complex which ratio average is range from 99.5 to 410.2 (Table 4). There are few samples have RPTR larger than 600 they have qiute different ratio distrbution. (Figure 5).

Num	For	RPTR distribution (%)				Average
		I	II	III	IV	
6	T_3x^4	3.4	80.1	16.0	0.5	332.7
7	T_3x^4	4.1	55.2	35.1	5.6	410.2
10	T_3x^4	33.9	58.4	8.0	0.2	247.9
15	J_2x	14.0	51.2	29.4	5.4	377.0
35	T_3x^2	9.0	63.2	26.1	1.7	350.9
39	J_2x	88.0	11.7	0.3	0.0	119.7
59	T_3x^4	34.3	64.1	1.6	0.0	235.0
60	T_3x^2	17.2	52.8	25.4	4.6	355.1
65	T_3x^4	93.8	6.2	0.0	0.0	99.5

I: RPTR < 200; II: RPTR 200~400; III: RPTR 400~600; IV: RPTR > 600

Table 4: Ratio of pore-throat radius data

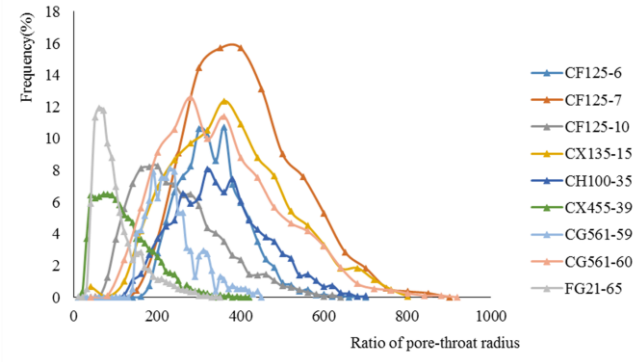

Figure 5: RPTR distributions of 8 samples

TechConnect Briefs 2017, TechConnect.org, ISBN 978-0-9975117-9-6

4 DISCUSSION

In WSD diagenesis continued for a long period of time. Some phenomena or configurations which we can observe by cast thin sections and SEM can reflect different types of diagenesis even their intensity. In this study, we use numbers of stylolite (Sty) to reflect intensity of compaction, cements including calcite (Ca), siliceous cement (Si), kaolinite (Ka) and chlorite (Ch) to reflect intensity of cementation, and amount of intergranular pore and intragranular pore space (PS) to reflect intensity of dissolution (Table 5).

Num	For	Sty	Ca (%)	Si (%)	Ka (%)	Ch (%)	PS (%)
6	T_3x^4	rare	4.0	2.0	2.0	/	rare
7	T_3x^4	6	3.0	4.0	2.0	3.0	rare
10	T_3x^4	/	7.5	1.5	1.5	rare	/
15	J_2x	7	6.0	/	2.0	/	rare
35	T_3x^2	5	8.1	1.0	1.9	3.9	rare
39	J_2x	rare	1.0	0.0	/	/	4.0
59	T_3x^4	6	2.0	3.0	1.8	3.0	/
60	T_3x^2	4	0.5	5.2	4.2	rare	rare
65	T_3x^4	rare	0.5	0.1	/	rare	2.0

Table 5 Types and intensity of diagensis of samples

Based on the results, we choose samples experienced different diagenesis to compare their porosity and permeability, so that we can conjecture how diagenesis controls physical properties through microscopic structures.

In tight sandstone reservoirs, strong compaction is the main factor of poor porosity bacause the compressive strength will reduce the pore space. Samples with more stylolites almost have lower porosity than others (27.02% in average).

From Table 2 and Table 3 we can conclude that the throat space is much narrower than pore body in each sample, which means compaction may not have that important influence on throat. So that cementation is the main reason of narrow throat, because the cements can block those throats. The samples with high cement contents (Sample 35, 60 and 15) have smaller throat radius (Table 3), which then lead to lower permeability (0.445×10^{-3} μm^2).

As for pore throat ralationship, there seems no obvious controlling factors. But some samples with rare pore space (sample 7 and 60) has higher RPTR. So we think it may attibute to dissolution only occurred in small part of whole sample. Because the pore fliud which can enrich pore space can not easily pass through throats to enlarge throat space.

5 CONCLUSION

In this study, we choose 8 samples from WSD to analyze microscopic pore structures and its controlling factors using several laboratory techniques, and the conclusions are as follows:

(1). The main pore types in WSD are intergranular pores and intragranular pores, their radius is from 100 to 150μm with similar distribution. Throats are much narrower than pores with an average less than 1μm, and their distributions are complex. Relationship between pore body and throat can be reflect by distribution and size of ratio of pore throat radius. Among 8 samples this ratio varies from 99.5 to 410.2, and the different distribution of this ratio also shows the complexness of microscopic pore structure in this area.

(2). Diagenesis controls microscopic pore structures and then lead to poor physical properties of the reserviors. Strong compaction made smaller pore space and then lower porosity; cementation caused the cements to block throat which decrease permeability of reservoirs; and dissolution made a larger disparity among pore body and throat, it is difficult to say it is better for physical properties or not. In actual situation, these diagenesis must together influce microscopic pore structures in a more complex way, which needs further study.

6 ACKNOWLEDGEMENTS

We are grateful for support by a National Natural Science Foundation Project (ZX20140137). We also thank China National Key Laboratories of Petroleum Resources and Prospecting for their sample analysis and experiments.

REFERENCES:

[1] R Wang, M Chen, "Characteristics and influencing factors of movable fluid in ultra-low permeability sandstone reservoir," Acta Petrolei Sinica, 29(4), 558-561, 2008.

[2] R Li, Z Wang, W Li, et al. "Multifractal Properties of Tight Rock Pore Structure Based on Thin Section," Journal of Xi'an Shiyou University (Natural Science Edition), 31(6), 66-71, 2016.

[3] Liu N, Nan J, et al. "Test method and characteristics for micro-pore throat structure of Chang7 tight sandstone reservoirs," Petrochemical Industry Application, 33(7), 7-13, 2014.

[4] B Bai, R Zhu, S Wu, et al. "Multi-scale method of Nano(Micro)-CT study on microscopic pore structure oftight sandstone of Yanchang Formation, Ordos Basin," Petroleum Exploration and Development, 40(3), 329-33, 2013.

[5] S Li, W Sun, L Wang, "Application of constant-rate mercury injection technology in reservoir pore structure study," Fault-Block Oil & Gas Field, 20(4), 485-487, 2013.

[6] J Ye, H Zeng. "Pooling conditions and exploration prospect of shale gas in Xujiahe formation in Western Sichuan Depression," Natural Gas Industry, 18-25, 2008.

[7] Z Luo, Y Wang. "Pore structures of oil gas reservior," Beijing: Petroleum Industry Press, 1986.